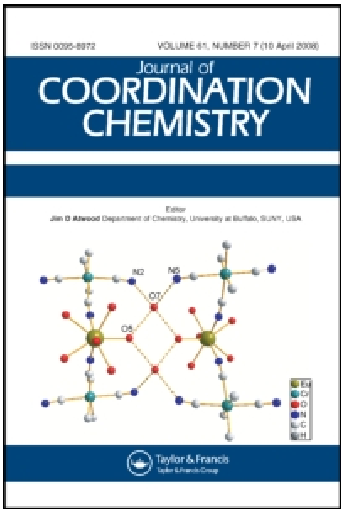

Journal of Coordination Chemistry
Publication details, including instructions for authors and subscription information:
http://www.informaworld.com/smpp/title~content=t713455674

A new linear-chain complex based on heptamolybdates with {Ce(H_2O)$_5$} linkers

Youzhi Fu[a]
[a] Department of Chemistry, Baicheng Teacher's College, Baicheng 137000, P.R. China

To cite this Article Fu, Youzhi(2010) 'A new linear-chain complex based on heptamolybdates with {Ce(H_2O)$_5$} linkers', Journal of Coordination Chemistry, 63: 11, 1856 — 1864, First published on: 25 June 2010 (iFirst)
To link to this Article: DOI: 10.1080/00958972.2010.494725
URL: http://dx.doi.org/10.1080/00958972.2010.494725

Journal of Coordination Chemistry
Vol. 63, No. 11, 10 June 2010, 1856–1864

A new linear-chain complex based on heptamolybdates with $\{Ce(H_2O)_5\}$ linkers

YOUZHI FU*

Department of Chemistry, Baicheng Teacher's College, Baicheng 137000, P.R. China

(*Received 18 December 2009; in final form 11 March 2010*)

A new linear-chain structure based on heptamolybdates with the linkage of $\{Ce(H_2O)_5\}$ units, $(C_6H_{13}N_4)_2(H_3O)[Ce(H_2O)_5Mo_7O_{24}]\cdot 4H_2O$ (**1**) has been synthesized and characterized by single crystal X-ray diffraction, IR spectroscopy, elemental analysis, and thermogravimetric analysis. Magnetic studies show strong spin–orbital coupling interactions and/or antiferromagnetic interactions within Ce(III) centers.

Keywords: Polyoxometalate; Linear-chain; Heptamolybdate; Cerium

1. Introduction

Polyoxometalates (POMs), a fascinating class of metal–oxygen cluster complexes with structural variety and interesting physicochemical properties, have been found to be extremely versatile inorganic building blocks with potential applications in catalysis, medicine, and materials [1–5]. Many transition metal and lanthanide cations have been introduced into the structure of POMs, forming new classes of materials with potential magnetic and luminescent properties [6–9]. Hill *et al.* [10] have used $NaH_3[SiW_{11}CeO_{39}]$ as the active site for the aerobic oxidation of formaldehyde. Also, Boglio *et al.* [11] discovered that $[\alpha_1\text{-}Ln(H_2O)_4P_2W_{17}O_{61}]$ can act as selective and recoverable Lewis acid catalyst. Sparked by the many applications for POM–Ln clusters, much interest has been focused on their rational synthesis and assembly. A few interesting studies on this POM–Ln cluster synthesis have been performed by Pope, Francesconi, Sécheresse, Yamase, Thouvenot, etc. [12–18]. However, most of them are based on heteropolyoxometalates (especially Keggin, Dawson, and Anderson-type) and their lacunary species. In contrast, there are only a few reports about lanthanide complexes based on isopolyoxometalates [19–21]. The potent antitumor activity of heptamolybdate anion makes it an excellent candidate for new material design. Because the primary structure of heptamolybdate anion often collapses when it is used as a precursor, POM–Ln materials based on heptamolybdate are rare and it remains a challenge to prepare new heptamolybdate-based POM–Ln materials.

---

*Email: fuyz112@163.com

Journal of Coordination Chemistry
ISSN 0095-8972 print/ISSN 1029-0389 online © 2010 Taylor & Francis
DOI: 10.1080/00958972.2010.494725

It has been reported that $[H_2Mo_{16}O_{52}]^{10-}$, a highly charged cluster anion, undergoes gradual decomposition and rearranges to a zigzag-shaped, 1-D anionic coordination polymer $(C_6H_{14}N_4)_{1.5}(C_7H_{17}N_5)_{0.5}[Na_2Mo_7O_{24}(H_2O)_5]\cdot 4H_2O$. When divalent transition metal cations in high concentration are introduced in this system, $[M_2(H_2O)_9Mo_7O_{24}]^{2-}$ (M = Fe(II) or Mn(II)) can be isolated [22]. Therefore, we are wondering what will happen if lanthanide metals are introduced instead. Here, we report the synthesis of a new heptamolybdate–Ln complex, $(C_6H_{13}N_4)_2(H_3O)\cdot[Ce(H_2O)_5Mo_7O_{24}]\cdot 4H_2O$ (**1**). The structure of **1** was characterized by single crystal X-ray diffraction, IR spectroscopy, elemental analysis, and thermogravimetric (TG) analysis. To the best of our knowledge, it is the first example of linear-chain structure complex based on heptamolybdates with the linkage of lanthanide metals.

2. Experimental

2.1. *Materials and methods*

Elemental analyses (C, H, and N) were performed on a Perkin Elmer 2400 CHN Elemental Analyzer. Mo and Ce were determined by a Leaman inductively coupled plasma (ICP) spectrometer. The IR spectra were obtained from 400 to 4000 cm^{-1} on an Alpha centaure FT/IR spectrophotometer using KBr pellets. TG analysis was performed on a Perkin Elmer TGA7 instrument in flowing N_2 with a heating rate of 5°C min^{-1}. The magnetic susceptibility measurements for **1** were carried out on polycrystalline samples using a Quantum Design MPMS-XL-5 SQUID magnetometer from 2 to 300 K with an applied field of 0.1 T. Diamagnetic corrections were estimated from Pascal's constants.

2.2. *Synthesis of 1*

Hexamethylenetetramine (HMTA) weighing 2.2 g was dissolved in 20 mL water and acidified with HCl (37%, 1.2 mL). Then 0.96 g of $Na_2MoO_4\cdot 2H_2O$ and 0.07 g of $Na_2S_2O_4$ were added with stirring. The obtained $[H_2Mo_{16}O_{52}]$ solution was kept overnight (12 h). Then 0.1 g of $Ce(NO_3)_3$ and 0.1 g of citric acid were added to the above solution and the pH was adjusted to 5.3 by 1 mol L^{-1} NaOH. The mixture was stirred for 1 h and then filtered. After 2 weeks, yellow block crystals were obtained which were washed with distilled water, filtered off, and dried in air (52% yield based on Mo). Elemental analysis: Calcd for $C_{12}H_{46}N_8CeMo_7O_{34}$ (%): Mo, 40.50; Ce, 8.45; C, 8.69; H, 2.80; and N, 6.76. Found (%): Mo, 40.55; Ce, 8.84; C, 8.41; H, 2.94; and N, 6.75. IR (KBr pellet): 3416(m), 1628(w), 1410(m), 1368(m), 1299(w), 1256(m), 1018(m), 985(m), 887(s), 832(s), 629(s), 571(s), and 415(s) cm^{-1}.

2.3. *X-ray crystallographic analysis*

The structure of **1** was determined by single crystal X-ray diffraction. A single yellow crystal with approximate dimensions of $0.30 \times 0.15 \times 0.08\ mm^3$ was mounted to the end

Table 1. Crystal data and structure refinement.

Empirical formula	$C_{12}H_{46}N_8CeMo_7O_{34}$
Formula weight	1658.27
Temperature (K)	296(2)
Wavelength (Å)	0.71073
Crystal system	Orthorhombic
Space group	*Pnma*
Unit cell dimensions (Å, °)	
a	23.687(4)
b	19.366(3)
c	8.5814(14)
α	90
β	90
γ	90
Volume (Å^3), Z	3936.5(11), 4
Calculated density ($g\,cm^{-3}$)	2.798
Absorption coefficient (mm^{-1})	3.407
$F(0\,0\,0)$	3192
Reflections collected	17,452
Independent reflections	3975 [$R(\text{int}) = 0.0555$]
Data/restraints/parameters	3975/0/309
Goodness-of-fit on F^2	1.052
Final R indices [$I > 2\sigma(I)$]^a	$R_1 = 0.0494$, $wR_2 = 0.1179$
R indices (all data)^a	$R_1 = 0.0659$, $wR_2 = 0.1256$

$^a R_1 = \Sigma||F_o| - |F_c||/\Sigma|F_o|$; $wR_2 = \Sigma[w(F_o^2 - F_o^2)^2]/\Sigma[w(F_o^2)^2]^{1/2}$.

of a glass fiber capillary. Crystal data for **1** were collected on a Bruker Smart CCD ApexII diffractometer with Mo-Kα monochromatic radiation ($\lambda = 0.71073$ Å) at 296 K and oscillation scans technique in the range $1.72 < \theta < 26.21°$. The structure was solved by direct methods and refined by full-matrix least-squares on F^2 using the *SHELXTL* crystallographic software package. The non-hydrogen atoms were refined anisotropically. The positions of hydrogens on carbon were calculated. Structure solution and refinement based on 3975 independent reflections with $I > 2\sigma(I)$ and 309 parameters gave $R_1(wR_2) = 0.0494$ (0.1179). In addition, Mo3, Mo4, and Mo5 in **1** are disordered over two locations. The occupancies for them over two sites are 0.5. Crystal data for **1** are summarized in table 1. Selected bond lengths are given in table 2 (Supplementary material).

3. Results and discussion

3.1. *Synthesis*

Complex **1** was prepared by the reaction of $[H_2Mo_{16}O_{52}]$ and $Ce(NO_3)_3$ in the presence of HMTA and citric acid. We have manipulated a number of variables such as pH, ligand, cation size and type, etc. Primary importance in the preparation of this complex is the introduction of a large excess of citric acid. Citric acid was chosen because it is effective in stabilizing lanthanide ions even in high-pH aqueous solution. Second, the organic cations play an important role in assembling this complex. Third, the pH of the system is also a vital factor in the syntheses of these compounds. Complex **1** could only be obtained at a precise pH of 5.3.

Table 2. Selected bond lengths (Å) for **1**.

Mo(1)–O(15)	1.702(6)	Mo(1)–O(16)	1.746(6)
Mo(1)–O(14)	1.926(6)	Mo(1)–O(3)	1.962(6)
Mo(1)–O(4)	2.136(2)	Mo(1)–O(7)	2.210(6)
Mo(2)–O(12)	1.710(6)	Mo(2)–O(13)	1.724(6)
Mo(2)–O(11)	1.943(6)	Mo(2)–O(14)	1.953(6)
Mo(2)–O(8)	2.168(2)	Mo(2)–O(7)	2.249(6)
Mo(3)–O(6)	1.723(9)	Mo(3)–O(5)	1.749(8)
Mo(3)–O(7)	1.890(6)	Mo(3)–O(7)$^{\#1}$	1.890(6)
Mo(3)–O(8)	2.205(8)	Mo(3)–O(4)	2.232(8)
Mo(4)–O(2)	1.707(8)	Mo(4)–O(1)	1.760(9)
Mo(4)–O(3)	1.914(6)	Mo(4)–O(3)$^{\#1}$	1.914(6)
Mo(4)–O(4)	2.129(8)	Mo(4)–O(5)	2.431(8)
Mo(5)–O(10)	1.704(9)	Mo(5)–O(9)	1.730(10)
Mo(5)–O(11)	1.923(6)	Mo(5)–O(11)$^{\#1}$	1.923(6)
Mo(5)–O(8)	2.144(8)	Ce(1)–O(2W)$^{\#1}$	2.504(7)
Ce(1)–O(2W)	2.504(7)	Ce(1)–O(3W)	2.507(9)
Ce(1)–O(1)$^{\#2}$	2.535(9)	Ce(1)–O(1W)	2.567(7)
Ce(1)–O(1W)$^{\#1}$	2.567(7)	Ce(1)–O(5)$^{\#2}$	2.577(9)
Ce(1)–O(16)	2.577(6)	Ce(1)–O(16)$^{\#1}$	2.577(6)

O(W): Oxygen atom from water molecule.
$^{\#1}$: $x, -y+1/2, z$; $^{\#2}$: $x, y, z+1$

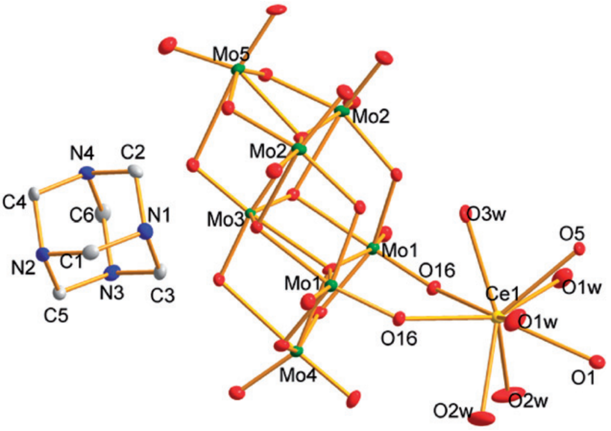

Figure 1. ORTEP view of **1** with thermal ellipsoids at 30%. Lattice waters are omitted for clarity.

3.2. *Structure description*

The structure of **1** is constructed from one $\{Ce(H_2O)_5\}^{3+}$ coordinating heptamolybdate anion, two protonated HMTA cations, one H_3O^+ cation, and four lattice waters (figure 1). According to the different coordinations of oxygen in $[Mo_7O_{24}]^{6-}$, it can be classified as Ot and Ob/c, where Ot is a terminal oxygen and Ob/c is an oxygen bridging between two or three molybdenums. Each Mo has two terminal oxygens except Mo3 located in the cavity of the bowl-shaped heptamolybdate cluster. The Mo–Ot distances vary from 1.702(6) to 1.730(10) Å, and the Mo–Ob/c bond lengths from 1.890(6) to 2.431(8) Å, while the Mo–O–Mo bond angles are in the range of 71.7(3)–163.1(3)°. The cerium cation is nine-coordinate with five waters (Ce–O 2.504(7)–2.567(7) Å), and four oxygen atoms from two $[Mo_7O_{24}]^{6-}$ anions (Ce–O 2.535(9)–2.577(6) Å). As observed

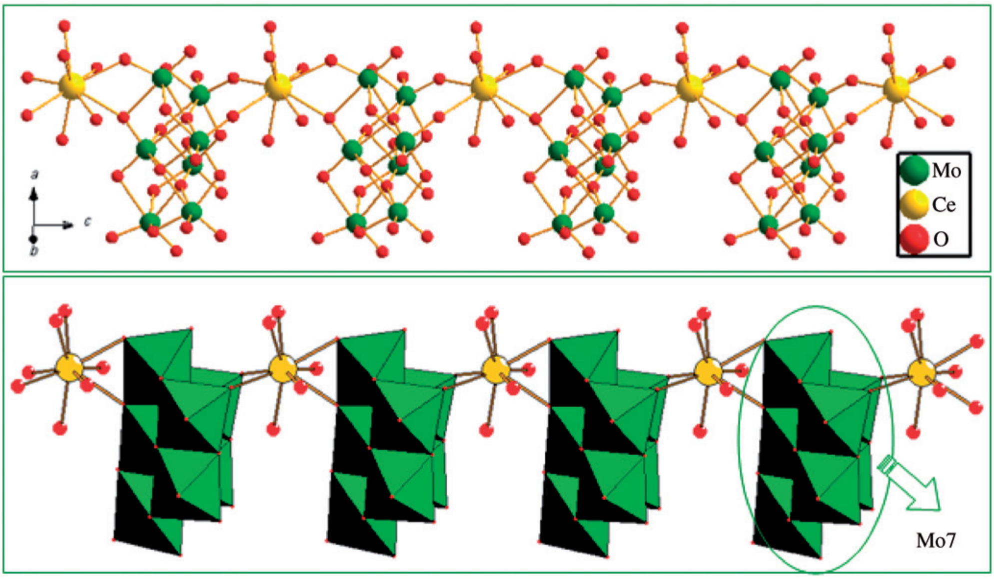

Figure 2. 1-D linear-chain of **1** along the *c*-axis. The heptamolybdate anions are linked with $\{Ce(H_2O)_5\}$ units.

for most lanthanide complexes of POMs, the Ce(III) is a distorted monocapped square antiprism. Bond valence sum (BVS) calculations [23] indicate that all the Mo centers are +6 and Ce center is +3 oxidation states (the calculated value of O atoms in $CeO_4(H_2O)_5$ is 0.394 for O2w, O2w$^{\#1}$; 0.323 for O5$^{\#2}$, O16, O16$^{\#1}$; 0.332 for O1w, O1w$^{\#1}$; 0.391 for O3w, and 0.362 for O1$^{\#2}$, respectively). The BVS values of all the oxygens are +2, which implies no protons in the structure of heptamolybdate.

In the structure of **1**, each heptamolybdate coordinates to two cerium cations and each cerium coordinates to two heptamolybdate anions, forming a linear-chain coordination polymer (figure 2). As shown in figure 3, in the *ac* plane, the chains are linked to form a 2-D layer through hydrogen bonds (O2w–H2wb $\cdots$ O9, 3.211 Å; O2w–H2wb $\cdots$ O10, 3.110 Å); while in the *ab* plane (figure 4), all the 2-D layers and cations are further connected through complex hydrogen bonding to form a 3-D supramolecular framework (O4w–H4wa $\cdots$ O13, 2.832 Å; O4w–H4wa $\cdots$ O15, 2.985 Å; O4w–H4wb $\cdots$ O1w, 2.792 Å; and O2w–H2wa $\cdots$ O4w, 3.021 Å). The hydrogen bond lengths for **1** are summarized in table 3.

Compared with the 1-D anionic coordination polymer $(C_6H_{13}N_4)_2[M_2(H_2O)_9 \cdot Mo_7O_{24}]_\infty$ (M = Fe(II) or Mn(II)) [22], the chain-like structure changes from zigzag to linear, due to the high coordination number and high oxophilicity of cerium. Also, by using a highly charged polyoxomolybdate anion, $[H_2Mo_{16}O_{52}]^{10-}$, as precursor, the heptamolybdate anion $[Mo_7O_{24}]^{6-}$ forms *in situ* gradually, which prevents decomposition of the heptamolybdate anion and reduces formation of precipitate after the addition of Ce ions. In comparison with two reported Ln/POMs complexes, $[Cu(en)_2]_2H_8[Gd(PW_{11}O_{39})_2] \cdot (H_2en)_{0.5} \cdot 3H_2O$ [24] and $[La(DMF)_7(H_2O)][PMo_{12}O_{40}] \cdot DMF \cdot (CH_3)_2NH$ [25], the structure of **1** is based on isopolymolybdates, and not on heteropolyanions. In contrast to an isolated cluster, $\{[Ce(Hbpy)(DMF)_5(H_2O)_2] \cdot [H_2W_{12}O_{40}]\}^{2-}$ [25], **1** shows a 1-D chain-like structure with a covalent linker $Ce(H_2O)_5$.

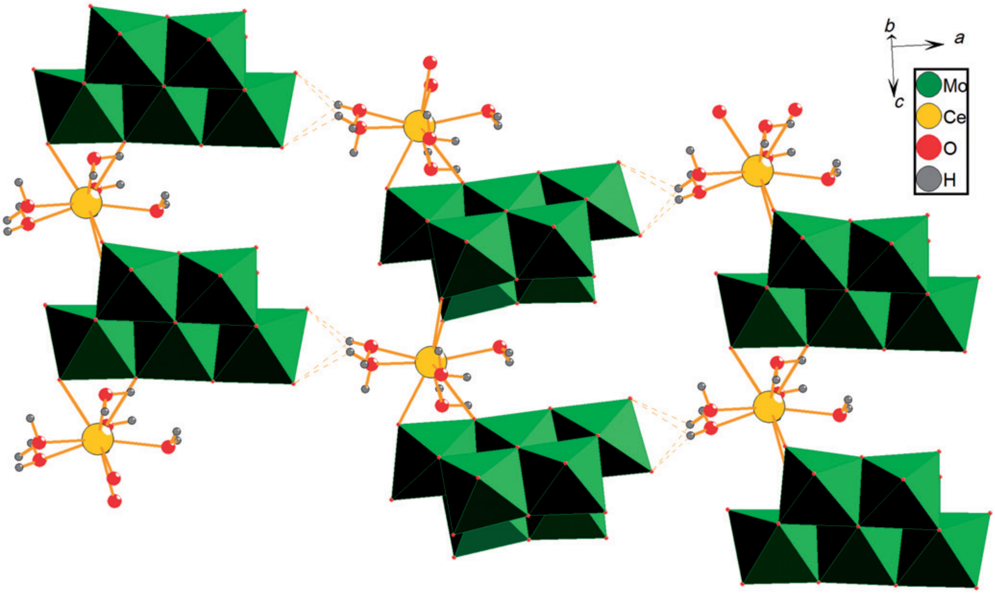

Figure 3. The 2-D layer structure of **1** linked with hydrogen bonds viewed along the *b*-axis.

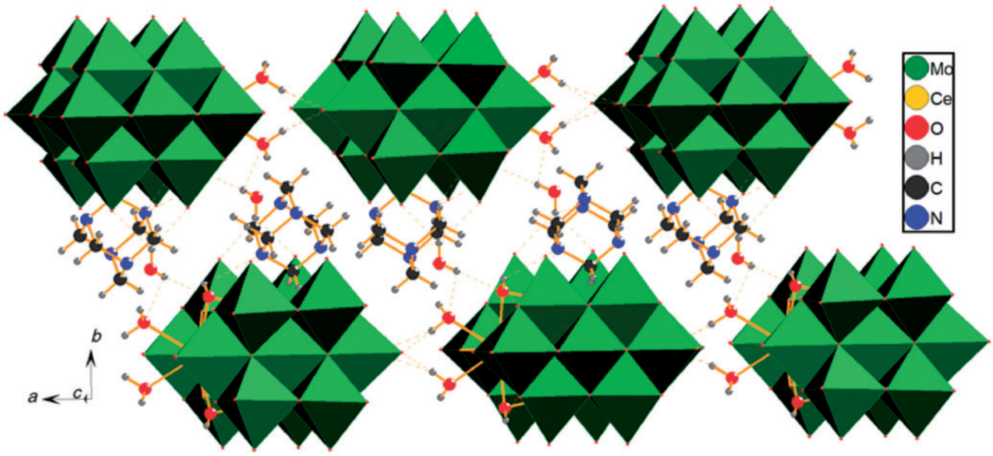

Figure 4. Combined polyhedral/ball-and-stick representation of 3-D supramolecular framework of **1** in the *ab* plane showing complex hydrogen-bonding.

3.3. *IR and TG analysis*

The IR spectrum of **1** shows characteristic vibrational features of heptamolybdates. Absorptions at 887 cm^{-1} are attributed to ν_{as}(Mo–Ot); other peaks falling in the range of 832–629 cm^{-1} are attributed to ν_{as}(Mo–Ob/c–Mo), which is similar to $[Mo_7O_{24}]^{6-}$ [26]. In addition, vibrational bands from 1018 to 1628 cm^{-1} can be assigned to vibrations of CH and NH in HMTA cations.

Table 3. Hydrogen bonds for **1**.

D–H···A	D–H (Å)	H···A (Å)	D···A (Å)	∠DHA (°)
O1w–H1wa···N3	0.88	2.32	2.796	114
O1w–H1wb···N3	0.89	2.30	2.796	113
O2w–H2wb···O9	0.96	2.54	3.211	127
O2w–H2wb···O10	0.96	2.19	3.110	161
O2w–H2wa···O4w	0.96	2.14	3.021	153
O4w–H4wa···O13	0.85	2.21	2.832	161
O4w–H4wa···O15	0.85	2.36	2.985	153
O4w–H4wb···O1w	0.85	2.02	2.792	150
O5w–H5wb···N4	0.88	2.04	2.841	151
O5w–H5wa···O4w	0.89	1.90	2.566	131

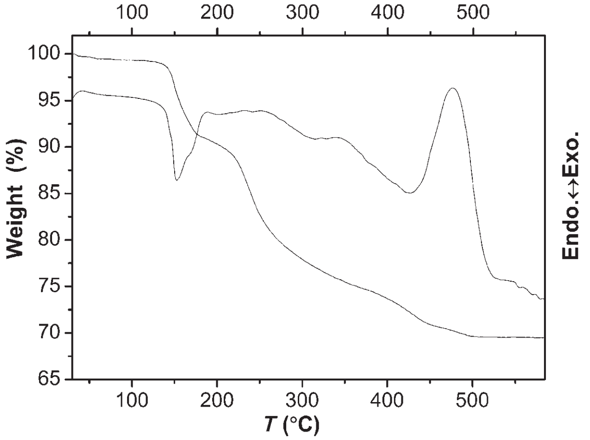

Figure 5. The TG curve of **1** measured from 30°C to 600°C in flowing N_2 with a heating rate of $5°C\,min^{-1}$.

The TG curve (figure 5) of **1** exhibits three main steps from 30°C to 600°C with a total loss of 30.7%, which corresponds to release of waters and HMTA cations. Weight loss of 10.2% between 100°C and 220°C corresponds to the removal of five lattice waters and five coordinated waters (calculated, 10.8%), giving an endothermic effect at 150°C. The second weight loss of 16.4% between 220°C and 420°C corresponds to loss of two HMTA cations (calculated, 17.0%). In DTA, the second endothermic stage, observed as several consecutive steps, is related to decomposition of HMTA cations. The last weight loss between 420°C and 500°C is attributed to the decomposition of the polyoxoanions. The strong exothermic peak in DTA at 475°C corresponds to polyanion backbone destruction.

3.4. *Magnetic studies*

Magnetic susceptibility measurements (300–2000) were performed on polycrystalline samples with an applied field of 1000 Oe using a Quantum Design MPMS XL–5 SQUID magnetometer. The diamagnetic correction of susceptibility data was carried

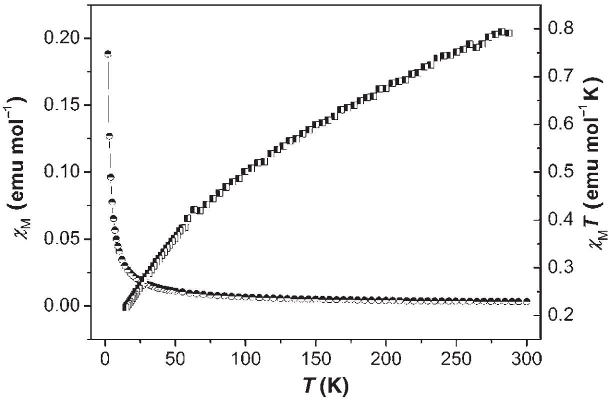

Figure 6. Temperature dependence of χ_M and $\chi_M T$ from 2 to 300 K for **1**.

out by Pascal's constants [27]. The temperature dependence of magnetic susceptibility χ_M and $\chi_M T$ for **1** is shown in figure 6. Upon cooling of the sample, the χ_M value increases, reaching a value of 0.19 emu K mol^{-1} at 2.0 K. The $\chi_M T$ value at room temperature is 0.79 emu K mol^{-1}, close to the expected value (0.80 cm^3 K mol^{-1}) for one isolated Ce(III) center ($S = 1/2$, $L = 3$, $^2F_{5/2}$). The $\chi_M T$ value decreases continuously with decreasing temperature, reaching a minimum of 0.22 emu K mol^{-1} at 2 K. The $1/\chi_M$ *versus* T plot (see in figure S1) for **1** could be fit with Curie–Weiss equation from 100 to 300 K, getting $C = 1.23$ emu K mol^{-1} and $\theta = -93.20$ K. As the temperature decreases from 100 to 2 K, the plot of $1/\chi_M$ *versus* T does not follow the Curie–Weiss law, indicating the occurrence of strong spin–orbital coupling interactions and/or antiferromagnetic interactions.

4. Conclusions

A new heptamolybdate–Ln coordination polymer with a linear-chain structure has been synthesized by conventional aqueous solution synthesis. Magnetic studies show strong spin–orbital coupling interactions and/or antiferromagnetic interactions between Ce(III) centers. The successful synthesis and isolation of **1** provides a feasible and effective synthetic route for constructing new POM–Ln materials.

Supplementary material

CCDC 736564 contains the supplementary crystallographic data for this article. These data can be obtained free of charge from the Cambridge Crystallographic Data Centre *via* www.ccdc.cam.ac.uk/data_request/cif. Some figures and IR spectrum for **1** are available. Supplementary data associated with this article can be found in the online version.

Acknowledgments

This work was financially supported by the National Natural Science Foundation of China (grants 20373009).

References

[1] M.T. Pope, A. Müller. *Angew. Chem. Int. Ed.*, **30**, 34 (1991).

[2] M.T. Pope. *Polyoxo Anions: Synthesis and Structure*, In *Comprehensive Coordination Chemistry II*, A.G. Wedd (Ed.), Vol. 4, p. 635, Elsevier Science, New York (2004).

[3] C.L. Hill. *Polyoxometalates: Reactivity*, In *Comprehensive Coordination Chemistry II*, A.G. Wedd (Ed.), Vol. 4, pp. 679–759, Elsevier Science, New York (2004).

[4] M.T. Pope, A. Müller (Eds). *Polyoxometalate Chemistry: From Topology via Self-Assembly to Applications*, Kluwer, Dordrecht, The Netherlands (2001).

[5] D.L. Long, E. Burkholder, L. Cronin. *Chem. Soc. Rev.*, **36**, 105 (2007).

[6] C. Benelli, D. Gatteschi. *Chem. Rev.*, **102**, 2369 (2002).

[7] T. Yamase. *Chem. Rev.*, **98**, 307 (1998).

[8] J.W. Zhao, H.P. Jia, J. Zhang, S.T. Zheng, G.Y. Yang. *Chem. Eur. J.*, **13**, 10030 (2007).

[9] S.S. Mal, M.H. Dickman, U. Kortz, A.M. Todea, A. Merca, H. Bögge, T. Glaser, A. Müller, S. Nelllutla, N. Kaur, J. Tol, N.S. Van Dalal, B. Keita, L. Nadjo. *Chem. Eur. J.*, **14**, 1186 (2008).

[10] O.A. Kholdeeva, M.N. Timofeeva, G.M. Maksimov, R.I. Maksimovskaya, W.A. Neiwert, C.L. Hill. *Inorg. Chem.*, **44**, 666 (2005).

[11] C. Boglio, G. Lemière, B. Hasenknopf, S. Thorimbert, E. Lacôte, M. Malacria. *Angew. Chem. Int. Ed.*, **45**, 3324 (2006).

[12] M. Sadakane, M.H. Dickman, M.T. Pope. *Angew. Chem. Int. Ed.*, **39**, 2914 (2000).

[13] R.C. Howell, F.G. Perez, S. Jain, W.D. Horrocks Jr, A.L. Rheingold, L.C. Francesconi. *Angew. Chem. Int. Ed.*, **40**, 4031 (2001).

[14] K. Fukaya, T. Yamase. *Angew. Chem. Int. Ed.*, **42**, 654 (2003).

[15] P. Mialane, A. Dolbecq, E. Rivière, J. Marrot, F. Sécheresse. *Eur. J. Inorg. Chem.*, 33 (2004).

[16] C. Bogilo, G. Lenoble, C. Duhayon, B. Hasenknopf, R. Thouvenot, C. Zhang, R.C. Howell, B.P. Burton-Pye, L.C. Francesconi, E. Lacote, S. Thorimbert, M. Malacria, C. Afonso, J.C. Tabet. *Inorg. Chem.*, **45**, 1389 (2006).

[17] X.K. Fang, T.M. Anderson, C. Benelli, C.L. Hill. *Chem. Eur. J.*, **11**, 712 (2005).

[18] B.S. Bassil, M.H. Dickman, U. Kortz. *Inorg. Chem.*, **46**, 2452 (2007).

[19] K. Burgemeister, D. Drewes, E.M. Limanski, I. Küper, B. Krebs. *Eur. J. Inorg. Chem.*, 2690 (2004).

[20] A. Kitamura, T. Ozeki, A. Yagasaki. *Inorg. Chem.*, **36**, 4275 (1997).

[21] N.V. Izarova, M.N. Sokolov, D.G. Samsonenko, A. Rothenberger, D.Y. Naumov, D. Fenske, V.P. Fedin. *Eur. J. Inorg. Chem.*, 4985 (2005).

[22] D.L. Long, P. Kögerler, L.J. Farrugia, L. Cronin. *Dalton Trans.*, 1372 (2005).

[23] L.D. Brown, D. Altermatt. *Acta Crystallogr. B.*, **41**, 244 (1985).

[24] Y.H. Liu, G.L. Guo, J.P. Wang. *J. Coord. Chem.*, **61**, 2428 (2008).

[25] H.L. Chen, Y. Ding, X.X. Xu, E.B. Wang, W.L. Chen, S. Chang, X.L. Wang. *J. Coord. Chem.*, **62**, 347 (2009).

[26] H.T. Evans, B.M. Gatehouse, P. Leverett. *J. Chem. Soc., Dalton Trans.*, 505 (1975).

[27] C.J. O'Conner. *Prog. Inorg. Chem.*, **29**, 203 (1982).